PCCP

PAPER

View Article Online
View Journal | View Issue

Cite this: *Phys. Chem. Chem. Phys.*, 2022, **24**, 17314

16OSTM10: a new open-shell transition metal conformational energy database to challenge contemporary semiempirical and force field methods†

Arseniy A. Otlyotov,[a] Andrey D. Moshchenkov,[ab] Luigi Cavallo *[c] and Yury Minenkov*[ad]

Received 10th April 2022,
Accepted 21st June 2022

DOI: 10.1039/d2cp01659a

rsc.li/pccp

A new database, 16OSTM10, containing 10 conformations for each of 16 non-multireference realistic-size open-shell transition metal (OSTM) complexes has been developed. Contemporary composite density functional theory (DFT) (PBEh-3c and B97-3c), semiempirical (PM6 and PM7) and the GFN*n*-xTB/FF family methods were examined against conventional DFT (PBE-D3(BJ), PBE0-D3(BJ), M06 and ωB97X-V) to reproduce the conformational energies. While good performance is observed for the conventional (the average Pearson correlation coefficient is ρ = 0.91) and composite DFT (average ρ = 0.93), semiempirical and force-field methods should still be used with caution for these challenging compounds. The corresponding average ρ values are 0.53 (PM6 and PM7), 0.75 (GFN1-xTB and GFN2-xTB) and 0.62 (GFN-FF). Accounting for the intramolecular dispersion interactions turned out to be crucial for 4 OSTM complexes bearing bulky substituents in close proximity to each other. The influence of the scalar relativistic effects on the conformational energies is negligible for the considered 3d metal species.

1. Introduction

Open-shell (OS) transition metal (TM) complexes are vital precursors for a number of industrial and academic applications. TM compounds act as catalysts in a number of important processes relevant to chemistry[1–5] and biology.[6] These complexes often possess magnetic anisotropy,[7,8] making them applicable as a base for promising information storage devices. To unravel their chemical and physical properties, molecular modeling is often required. The latter is anything but a simple task as, apart from the problems stemming from the complex electronic structures,[9–14] many open-shell transition metal complexes bear bulky flexible ligands giving rise to conformational issues that have to be dealt carefully.[15–22] The crucial role of a thorough conformational analysis in the investigations of the reaction pathways driven by transition metal catalysts has been revealed in a recent study by Vitek *et al.*[18]

Contemporary computational chemistry offers a number of methods for conformational sampling/search ranging from cheap force-fields (FF)[23–26] to the high-level DFT and *ab initio* approaches.[27] An efficient method should provide desirable accuracy to ensure the realistic PES, but still possess low computational cost to cover a larger part of the conformational space. The development, further tuning and validation of potential energy function approaches require databases containing the spatial structures and relative conformational energies of the relevant compounds. Such datasets have been recently generated for flexible organic molecules[28] and closed-shell TM complexes[15,16] and used for the systematic investigations of the performance of contemporary semiempirical (SE), force-field and composite DFT methods. The conformational energies obtained with SE methods PM6*/PM7 were found to be in poor agreement with their DFT[15,16] and high-level DLPNO-CCSD(T)[28] counterparts. A better, yet moderate performance is demonstrated by GFN*n*-xTB SE methods.[15,28] According to Bursch *et al.*,[16] reasonable conformational energies of closed-shell TM complexes can be obtained from single-point energy (SPE) calculations using a composite density functional

[a] *N. N. Semenov Federal Research Center for Chemical Physics RAS, Kosygina Street 4, 119991, Moscow, Russia. E-mail: yury.minenkov@chph.ras.ru*
[b] *Higher Chemical College of the Russian Academy of Sciences, Dmitry Mendeleev University of Chemical Technology of Russia, Miusskaya sq. 9, 125047, Moscow, Russia*
[c] *KAUST Catalysis Center (KCC), King Abdullah University of Science and Technology, Thuwal, 23955-6900, Saudi Arabia. E-mail: luigi.cavallo@kaust.edu.sa*
[d] *Joint Institute for High Temperatures, Russian Academy of Sciences, 13-2 Izhorskaya Street, Moscow, 125412, Russia*

† Electronic supplementary information (ESI) available: Tabulated values forming the basis of Fig. 2–8, T1/T2 diagnostic values, FOD plots (Fig. S1–S6), Cartesian coordinates (Å) of PBE-D3(BJ)/def2-svp optimized spatial structures, and total single-point conformational energies: M06/def2-tzvp, PBE0-D3(BJ)/def2-tzvp, PBE-D3(BJ)/def2-tzvp, ωB97X-V/def2-tzvp, PBEh-3c, B97-3c, PM6, PM7, GFN1-xTB, GFN2-xTB, and GFN-FF. See DOI: https://doi.org/10.1039/d2cp01659a

method (*e.g.* B97-3c) performed on GFN2-xTB optimized geometries.

However, there have been no systematic investigations on the performance of fast SE, FF and composite DFT approaches for the conformational energies of open-shell TM complexes. To fill this gap, we first develop a new database, 16OSTM10, containing 10 energetically and structurally diverse conformations for each of 16 realistic-size open-shell transition metal complexes. Second, we examine well-established DFT methods (PBE-D3(BJ), PBE0-D3(BJ), M06, and ωB97X-V), their recent composite versions (PBEh-3c and B97-3c) and contemporary SE (PM6, PM7, and GFN*n*-xTB) and FF (GFN-FF) schemes. The influence of scalar relativistic effects and intramolecular dispersion interactions on the conformational energies is discussed. A detailed statistical analysis was performed to find out the relative performance of the tested groups of methods.

Within a broader chemical context, we believe that the 16OSTM10 database together with its previously developed analogues for closed-shell TM complexes[15,16] can serve as a prototype for the machine-learning (ML) training tool to yield high-quality conformational energies. Very recently, the use of trained artificial neural networks (ANNs) was demonstrated[29] to predict adiabatic spin splitting and ionization potentials of CCSD(T) quality at significantly reduced computational cost.

2. Methods

2.1 Compound selection

The initial structures of transition metal complexes were retrieved from the online version of the Cambridge Structural Database (CSD).[30] The pre-selection procedure was based on the following criteria:

(1) A compound should contain a first row transition metal and (potentially) possess an open-shell electron configuration.

(2) A compound has at least 5 rotatable bonds implying a conformational manifold.

(3) A compound is of fundamental or applied scientific interest.

2.2 Conformer generation

The spatial structures of all the pre-selected compounds were optimized using the ORCA 5.0.2 suite of programs[31,32] at the PBE-D3(BJ)/def2-svp level of theory. Electronic states with relevant multiplicities, namely, 1, 3, 5 for species with an even number of electrons and 2, 4, 6 in the case of an odd number of electrons, were considered. The energies of the optimized structures were re-evaluated at the PBE0-D3(BJ)/def2-tzvp level of theory. Only the species with non-singlet ground electronic states were selected for further processing. As the present study focuses on the applicability of single-reference methods for the calculation of conformational energies, compounds exhibiting significant multireference character were excluded. A well-established T1/T2 diagnostics based on the DLPNO-CCSD(T)/cc-pVDZ calculations was utilized for this purpose. In the case of $T_1 > 0.025$ and/or $T_2 > 0.15$, a compound was considered to be of significant multireference character and excluded from the selection. For the species (FUDNIB, UZEYAA, FIYMEI, LIBLEN, YIKLUC and AJOMIX) for which DLPNO-CCSD(T) turned out not to be accessible, we performed FOD diagnostics[33] (see Fig. S1–S6, ESI†). Finally, 16 open-shell transition metal compounds satisfying all the above-mentioned criteria were chosen to form our database. Their structures with CSD names are given in Fig. 1.

In the second step, the sets containing 30–35 spatially diverse conformations of the selected compounds were automatically generated using an in-house code. All these structures were pre-optimized using a computationally undemanding approximation combining the standard PBE functional[34,35] and double-ζ quality Gaussian-type nuclei-centered λ1 basis sets (their detailed compositions are given in the ESI†)[36] as implemented in the Priroda code[37] and then checked to exclude possible duplicates. Our experience[28] suggests the PBE/λ1 approach to be suitable for the cheap preliminary optimizations. The spatial structures of the survived unique conformations were optimized at the PBE-D3(BJ)/def2-svp level of theory and further used for the calculations of the conformational energies (Section 2.3).

2.3 Examined methods for the calculations of conformational energies

A set of computationally efficient quantum-chemical approaches was used to obtain the conformational energies. First, we should note that the high-level DLPNO-CCSD(T1)/CBS method[38–40] often used to obtain accurate reference conformational energies turned out to be prohibitively expensive for many species containing up to 200 atoms. As dispersion-corrected DFT methods provide reliable conformational energies,[15] these have been used as references. To be unbiased, reference conformational energies were obtained with all-electron triple-ζ def2-tzvp basis sets[41] and four DFT functionals including standard PBE[34,35] and PBE0[42] complemented by D3(BJ) Grimme's dispersion correction,[43,44] hybrid meta-GGA M06[45] and range-separated hybrid ωB97X-V[46] functionals. In order to reveal the influence of scalar relativistic effects on the conformational energies we performed additional single-point (SP) calculations utilizing PBE functional and triple-ζ quality Gaussian-type nuclei-centered λ2 basis sets (see the ESI† for their detailed compositions)[36] with and without the Dyall scalar relativistic Hamiltonian[47] as implemented in the Priroda code.[37] This method accounts for the scalar relativistic effects, while spin–orbit coupling is neglected. The impact of dispersion interactions was evaluated by adding –D3(BJ) dispersion energy corrections[43,44] to the total PBE/λ2 electronic energies.

As practical conformational sampling prioritizes not only accuracy, but also computational efficiency, we have investigated the performance of the recently developed composite methods PBEh-3c[48] and B97-3c.[49] The cheapest approaches to obtain conformational energies are various semiempirical and force field methods. In the present contribution we examine the standard PM6[50] and PM7[51] SE methods as implemented in the MOPAC2016 program[52] and contemporary GFN*n*-xTB/FF[53–55] family of methods with use of the xtb 6.4.1 code.[56]

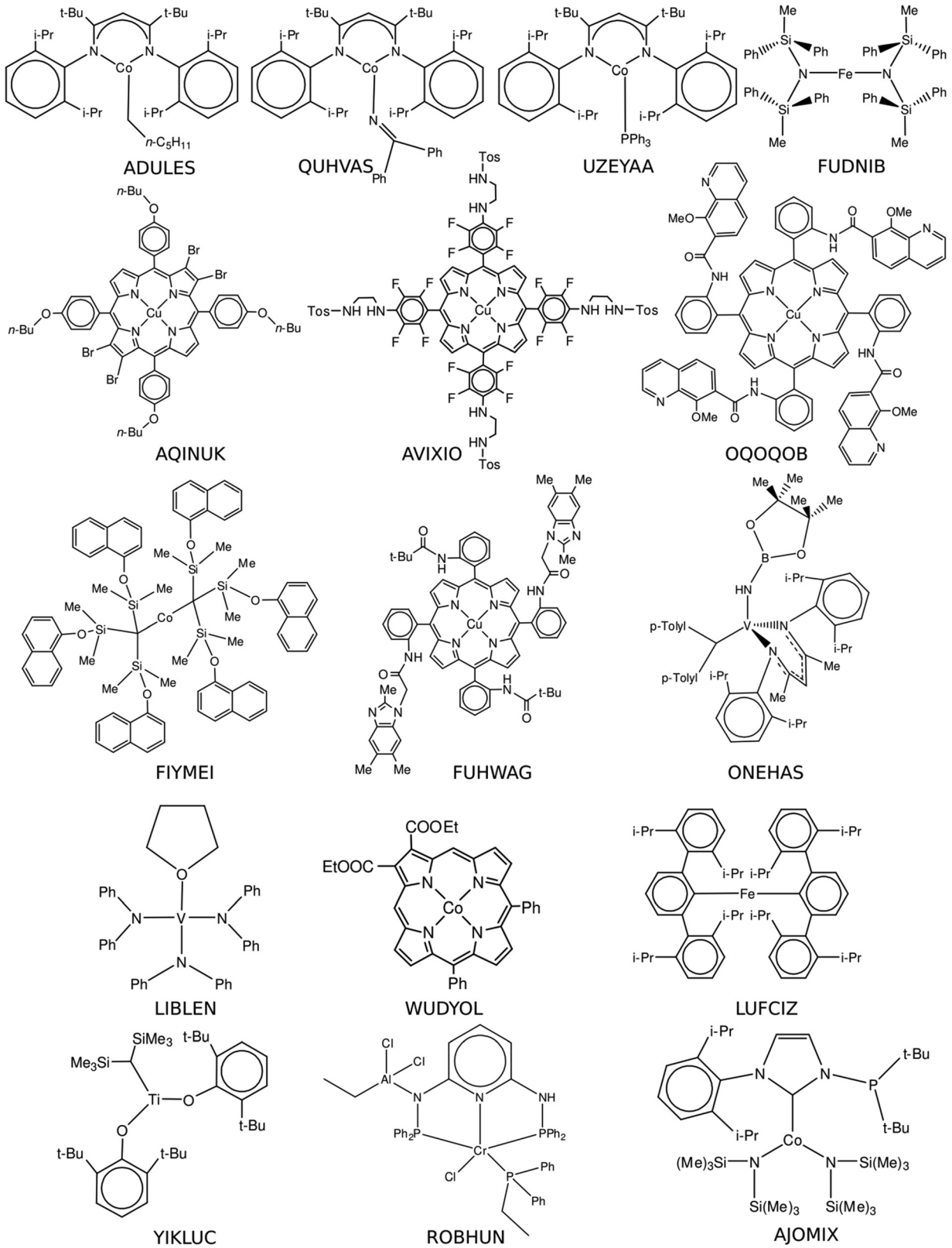

Fig. 1 16OSTM10 database comprising open-shell transition metal complexes with their CSD names.

3. Results and discussion

3.1 Comparison of the relative conformational energies

The quantitative comparison of the conformational energies calculated with different methods was based on the Pearson inter-correlation coefficients:

$$\rho(X, Y) = \frac{\sum_{i=1}^{n}(E_{x,i} - \overline{E_x})(E_{y,i} - \overline{E_y})}{\sqrt{\sum_{i=1}^{n}(E_{x,i} - \overline{E_x})^2(E_{y,i} - \overline{E_y})^2}}$$

where X and Y are the examined electronic structure methods, E_i are the relative conformational energies, and $\bar{E}$ are the average conformational energies for a given method. The positive ρ values close to 1 indicate a strong correlation between the tested methods, while negative ρ values close to -1 signify an anti-correlation.

Mean absolute error (MAE) was also used to quantify the difference between absolute conformational energies according to the formula:

$$\mathrm{MAE}(X, Y) = \frac{\sum_{i=1}^{n}|E_i(X) - E_i(Y)|}{n}$$

where X and Y are the examined electronic structure methods, n is the number of conformations for the compound (in our case n = 10), and E_i are the relative conformational energies.

For the conventional DFT functionals (PBE-D3(BJ), PBE0-D3(BJ), M06 and ωB97X-V), the mean Pearson correlation coefficients were calculated as follows: (1) the ρ values for the examined functional and each of the 3 remaining functionals were averaged for each compound; (2) the obtained values were averaged over all 16 OSTM complexes.

In the case of the composite DFT (PBEh-3c and B97-3c), semiempirical methods (PM6 and PM7) and the methods belonging to the GFN*n*-xTB/FF family (GFN1-xTB, GFN2-xTB and GFN-FF), the mean Pearson coefficients for each compound were obtained by averaging of the four ρ values calculated for the examined method and each of the conventional DFT functionals (PBE-D3(BJ), PBE0-D3(BJ), M06 and ωB97X-V).

MAEs were calculated in the same fashion as the Pearson correlation coefficients for all the examined electronic structure methods.

In the case of the YIKLUC complex, the GFN1-xTB method produced unreasonable results and this set of values was excluded from statistical analysis. A similar problem was previously mentioned for some TM complexes from the compilation of Bursch *et al.*[16]

3.1.1 Conventional DFT methods. As expected, conventional DFT functionals (PBE-D3(BJ), PBE0-D3(BJ), M06 and ωB97X-V) produce conformational energies satisfactorily correlated with one another (Fig. 2). Based on the Pearson coefficient ρ_{avg} = 0.91, averaged over the four examined methods, we will further consider the $\rho > 0.9$ values as indicators of the good correlation between the tested methods. Average mean absolute errors (MAE) for a conformational energy of 1.2 kcal mol^{-1} obtained for PBE, PBE0 and M06 functionals can be considered as acceptable, bearing in mind the large size of the OSTM complexes. A MAE of 1.5 kcal mol^{-1} and a relatively low mean correlation coefficient ρ = 0.87 with the 3 other methods were obtained for ωB97X-V, but we also include it in the set of the reference DFT functionals to be unbiased. Overall, these results additionally corroborate the protocol suggested in our previous work,[15] proving well-established DFT methods to be a reliable source of the conformational energies.

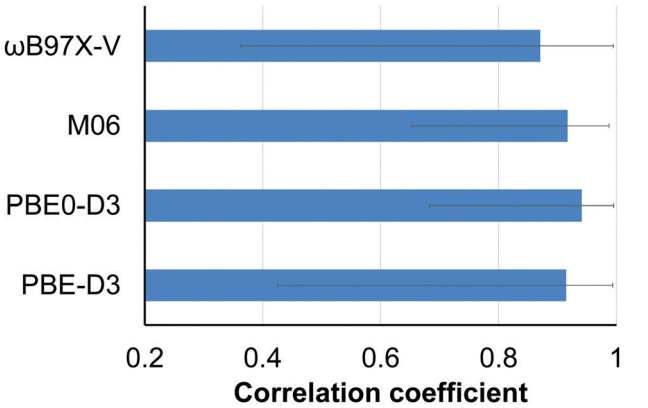

Fig. 2 Mean Pearson correlation coefficients (ρ) for the examined conventional DFT functional and each of the 3 remaining functionals, averaged over 16 OSTM complexes. The solid bars indicate the average ρ values, and the ends of the solid lines at each bar give the lowest and the largest values.

However, several two-coordinate complexes (LUFCIZ, FIYMEI and FUDNIB) remain challenging for the tested conventional methods, revealing low correlation coefficients (ρ = 0.53–0.82) and large (up to 4.5 kcal mol^{-1}) MAEs, and apparently require more sophisticated theoretical treatment.[57,58]

3.1.2 Composite DFT methods. Recently developed composite approaches like PBEh-3c and especially B97-3c were found to reproduce conformational energies highly correlated with the set of the conventional DFT functionals (see Fig. 3). The mean Person correlation coefficients for these methods averaged over all compounds are ρ = 0.90 and 0.95 for PBEh-3c and B97-3c, respectively. Low average MAEs of *ca.* 1.0 kcal mol^{-1} for both composite DFT functionals additionally indicate their good performance.

The worst correlation for AJOMIX stems from the narrow (0–3.3 kcal mol^{-1}) span in the absolute conformational energies for this compound. The conformational energies for LUFCIZ, FIYMEI and FUDNIB also exhibit a moderate correlation similar to the case of the conventional DFT methods (Section 3.1.1).

3.1.3 Semiempirical PM6 and PM7 methods. Computationally cheap SE PM6 and PM7 methods perform moderately for the most considered species. The low correlation ρ_{avg} = 0.51 (PM6), 0.55 (PM7), or even anti-correlation (AQINUK and FIYMEI) with the standard DFT functionals once again[15] admonishes to use these methods with caution for the conformational sampling of transition metal compounds. The largest error intervals for LUFCIZ, FIYMEI, AJOMIX and FUDNIB (Fig. 4) reflect the low correlation between the reference DFT methods for these compounds (see Section 3.1.1).

3.1.4 GFN*n*-xTB/FF family of methods. The contemporary SE methods GFN1-xTB and GFN2-xTB produce conformational

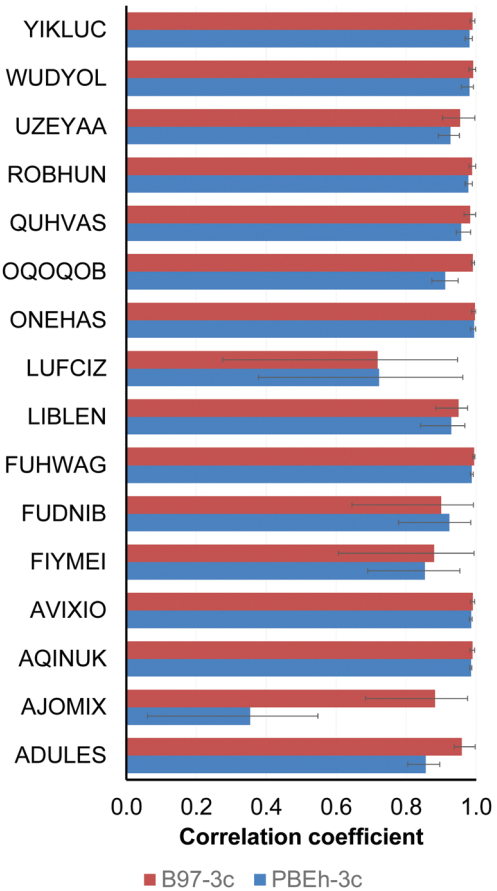

Fig. 3 Mean Pearson correlation coefficients (ρ) between composite (PBEh-3c and B97-3c) and standard (PBE-D3(BJ), PBE0-D3(BJ), M06 and ωB97X-V) DFT conformational energies. The solid bars indicate the average ρ values, and the ends of the solid lines at each bar give the lowest and the largest values.

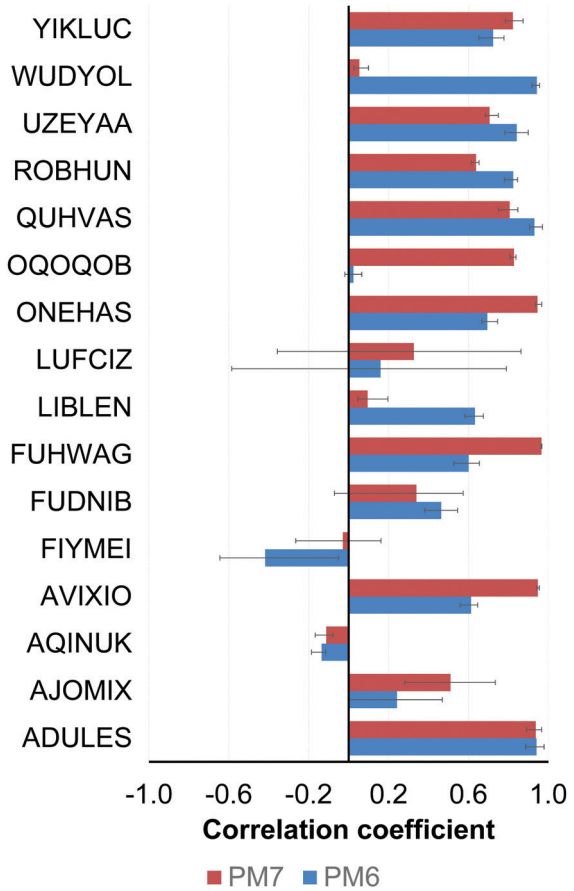

Fig. 4 Mean Pearson correlation coefficients (ρ) between semiempirical (PM6 and PM7) and standard (PBE-D3(BJ), PBE0-D3(BJ), M06 and ωB97X-V) DFT conformational energies. The solid bars indicate the average ρ values, and the ends of the solid lines at each bar give the lowest and the largest values.

energies better correlated with their reference DFT counterparts as compared to their PM6 and PM7 competitors. Mean Pearson correlation coefficients are ρ = 0.72 (GFN1-xTB) and 0.79 (GFN2-xTB). Some compounds (AQINUK, LIBLEN and LUFCIZ) remain challenging for both methods. Despite the relatively good ranking of the conformations (Fig. 5), an average MAE between GFN2-xTB and standard DFT methods is 2.4 kcal mol^{-1}, which is larger as compared to the composite DFT approaches. The force-field method GFN-FF is a worse performer with the mean ρ = 0.62.

3.1.5 Recommendations. The choice of the method for the conformational sampling is often a compromise between the desired accuracy and computational efficiency. The accuracy of each method is represented (Fig. 6) by the common statistical measures: median, first ($Q1$) and third ($Q3$) quartile values. The computational efficiency was estimated in terms of the relative time per 1 SCF iteration at the same computer architecture (Fig. 7). Among the examined conventional and composite DFT methods, B97-3c is the least computationally demanding, yet accurate. It thus can be a good tool for the conformational analysis of open-shell TM complexes, in line with their closed-shell analogues.[16]

Very fast semiempirical and force-field methods should be used with caution and proper validation for a target compound as they are characterized by large interquartile $Q1$/$Q3$ ranges as compared to the conventional and composite DFT (Fig. 6). Comparison of the NDDO PM6/7 methods with their tight-binding GFN counterparts in Fig. 6 illustrates a clear progress in semiempirical method development, still leaving them computationally affordable.

3.2 Impact of scalar relativistic effects on the conformational energies

For the 3d-metal species considered in this work relativistic effects start to be relevant.[59] In order to quantify their influence on the conformational energies, we performed separate calculations with and without the Dyall scalar-relativistic Hamiltonian (see Section 2.3). Accounting for the relativistic effects slightly (less than 0.4 kcal mol^{-1}) changes the absolute values of the relative conformational energies, but not the ranking of the conformations (ρ = 1.00) for all the considered compounds. This conclusion is true with and without *a posteriori* D3(BJ) dispersion correction added to the DFT energies.

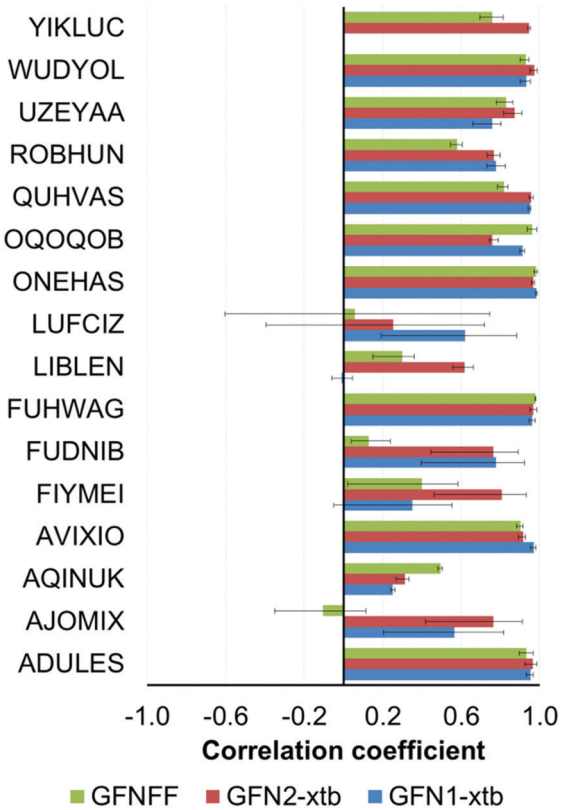

Fig. 5 Mean Pearson correlation coefficients (ρ) between GFNn-xTB/FF and standard (PBE-D3(BJ), PBE0-D3(BJ), M06 and ωB97X-V) DFT conformational energies. The solid bars indicate the average ρ values, and the ends of the solid lines at each bar give the lowest and the largest values.

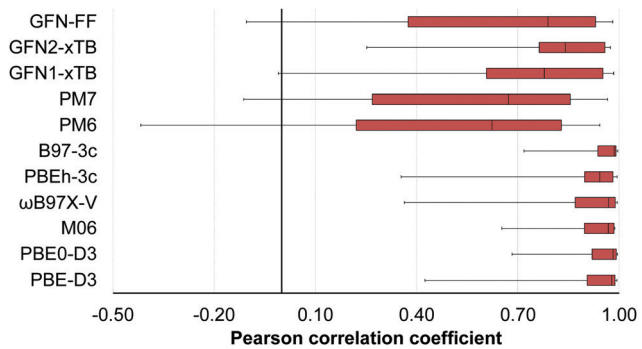

Fig. 6 Pearson correlation coefficients (ρ) for the examined methods: the left and right sides of the boxes correspond to the first ($Q1$) and third ($Q3$) quartiles, respectively. The vertical solid line inside each box gives the median ρ value. The whiskers give the lowest and largest ρ values for each method.

3.3 Influence of dispersion interactions on the conformational energies

Intramolecular dispersion interactions play a crucial role for many compounds of the 16OSTM10 compilation (Fig. 8). It becomes immediately clear from the selected correlation coefficients between PBE/λ2 and PBE-D3(BJ)/λ2 energies: ρ = −0.03 (AVIXIO), ρ = 0.36 (OQOQOB), ρ = 0.43 (FIYMEI),

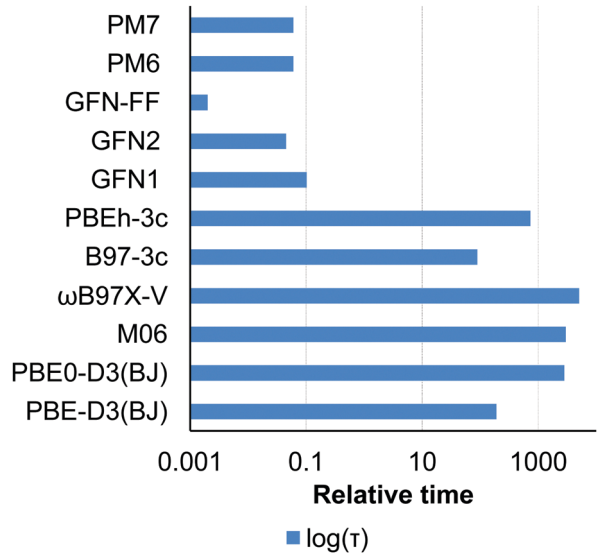

Fig. 7 Relative time for 1 SCF iteration performed with different methods for a conformation of LIBLEN. The logarithmic scale is used.

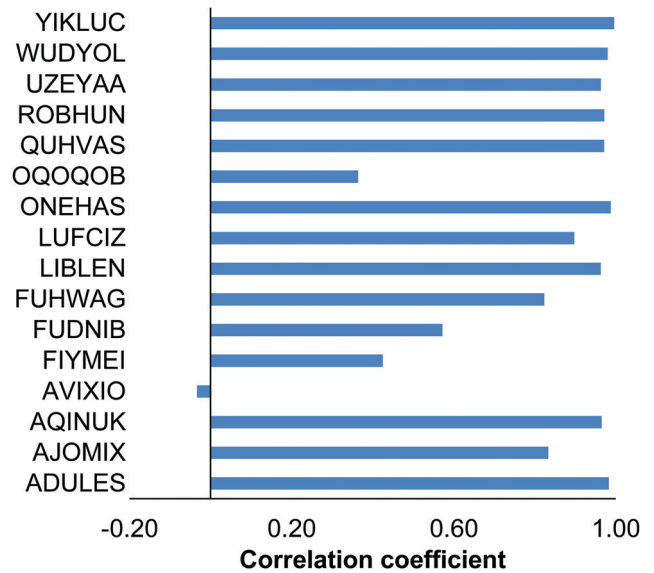

Fig. 8 Pearson correlation coefficients for the conformational energies obtained with (PBE-D3(BJ)/λ2) and without (PBE/λ2) accounting for the intramolecular dispersion interactions.

ρ = 0.57 (FUDNIB). Low correlation for these compounds can be explained by a major impact of the non-covalent interactions between their bulky substituents (see Fig. 1) located in the close proximity to each other. Overall, the obtained results indicate that conformational analysis performed without accounting for the dispersion interactions can lead to even qualitatively erroneous results.

4. Conclusions

A new database, 16OSTM10, containing 10 conformations for each of 16 realistic-size open-shell transition metal complexes

has been developed. Contemporary composite DFT, semiempirical and force-field methods have been examined against a set of conventional DFT methods (PBE-D3(BJ), PBE0-D3(BJ), M06 and ωB97X-V) in reproducing the relative conformational energies of the PBE-D3(BJ)/def2-svp optimized spatial structures. Similar to their closed-shell analogues, open-shell transition metal complexes remain challenging for PM6/PM7 semiempirical methods exhibiting the lowest Pearson correlation coefficients with the standard DFT methods. Significantly better performance was achieved for the GFN2-xTB semiempirical method, but still with particular failures for some compounds. The conformational energies obtained with the composite DFT methods B97-3c and PBEh-3c correlate well with their standard DFT counterparts. The recommendation to use the B97-3c approach for the reasonable single-point energies made in ref. 16 for the closed-shell species can be transferred to the open-shell ones.

Accounting for the relativistic effects results in a slight shift of the absolute conformational energies, but has no influence on the ranking of the conformations. The influence of the intramolecular dispersion interactions on the conformational energies is much more pronounced.

Author contributions

The manuscript was written through contributions of all authors. All authors have given approval to the final version of the manuscript.

Conflicts of interest

There are no conflicts to declare.

Acknowledgements

This work was financially supported by the grant of the President of the Russian Federation (''The development of an efficient approach for prediction of the properties of the open-shell organometallic compounds'', project MK-176.2022.1.3). L. C. gratefully acknowledges the financial support from King Abdullah University of Science and Technology (KAUST). For computer time, this research used the resources of the Supercomputing Laboratory at King Abdullah University of Science and Technology (KAUST) in Thuwal, Saudi Arabia and the Joint Supercomputer Center of RAS in Moscow, Russia.

Notes and references

1 F. Allouche, D. Klose, C. P. Gordon, A. Ashuiev, M. Wörle, V. Kalendra, V. Mougel, C. Copéret and G. Jeschke, Low-Coordinated Titanium(III) Alkyl—Molecular and Surface—Complexes: Detailed Structure from Advanced EPR Spectroscopy, *Angew. Chem., Int. Ed.*, 2018, **57**, 14533–14537.
2 Z. H. Qi and J. Ma, Dual Role of a Photocatalyst: Generation of Ni(0) Catalyst and Promotion of Catalytic C-N Bond Formation, *ACS Catal.*, 2018, **8**, 1456–1463.
3 J. Yang and T. D. Tilley, Efficient hydrosilylation of carbonyl compounds with the simple amide catalyst [Fe{N(SiMe3)2}2], *Angew. Chem., Int. Ed.*, 2010, **49**, 10186–10188.
4 A. Galindo, DFT Studies on the Mechanism of the Vanadium-Catalyzed Deoxydehydration of Diols, *Inorg. Chem.*, 2016, **55**, 2284–2289.
5 L. J. Clouston, V. Bernales, R. K. Carlson, L. Gagliardi and C. C. Lu, Bimetallic Cobalt-Dinitrogen Complexes: Impact of the Supporting Metal on N_2 Activation, *Inorg. Chem.*, 2015, **54**, 9263–9270.
6 A. Decker and E. I. Solomon, Dioxygen activation by copper, heme and non-heme iron enzymes: Comparison of electronic structures and reactivities, *Curr. Opin. Chem. Biol.*, 2005, **9**, 152–163.
7 P. C. Bunting, M. Atanasov, E. Damgaard-Møller, M. Perfetti, I. Crassee, M. Orlita, J. Overgaard, J. Van Slageren, F. Neese and J. R. Long, A linear cobalt(II) complex with maximal orbital angular momentum from a non-Aufbau ground state, *Science*, 2018, **362**, eaat7319.
8 W. A. Merrill, T. A. Stich, M. Brynda, G. J. Yeagle, J. C. Fettinger, R. De Hont, W. M. Reiff, C. E. Schulz, R. D. Britt and P. P. Power, Direct spectroscopic observation of large quenching of first-order orbital angular momentum with bending in monomeric, two-coordinate Fe(II) primary amido complexes and the profound magnetic effects of the absence of Jahnand- and Renner-Teller distortions, *J. Am. Chem. Soc.*, 2009, **131**, 12693–12702.
9 W. Jiang, N. J. Deyonker and A. K. Wilson, Multireference character for 3d transition-metal-containing molecules, *J. Chem. Theory Comput.*, 2012, **8**, 460–468.
10 K. Pierloot, Transition metals compounds: Outstanding challenges for multiconfigurational methods, *Int. J. Quantum Chem.*, 2011, **111**, 3291–3301.
11 A. L. Tchougreeff and M. B. Darkhovskii, in *Progr. Theor. Chem. Phys.*, Springer, Dordrecht, 2006, pp. 451–505.
12 I. B. Bersuker, *Electronic Structure and Properties of Transition Metal Compounds: Introduction to the Theory*, John Wiley and Sons, 2nd edn, 2010.
13 M. Atanasov and C. A. Daul, Modeling properties of molecules with open d-shells using density functional theory, *C. R. Chim.*, 2005, **8**, 1421–1433.
14 J. Wang, S. Manivasagam and A. K. Wilson, Multireference Character for 4d Transition Metal-Containing Molecules, *J. Chem. Theory Comput.*, 2015, **11**, 5865–5872.
15 Y. Minenkov, D. I. Sharapa and L. Cavallo, Application of Semiempirical Methods to Transition Metal Complexes: Fast Results but Hard-to-Predict Accuracy, *J. Chem. Theory Comput.*, 2018, **14**, 3428–3439.
16 M. Bursch, A. Hansen, P. Pracht, J. T. Kohn and S. Grimme, Theoretical study on conformational energies of transition metal complexes, *Phys. Chem. Chem. Phys.*, 2021, **23**, 287–299.
17 K. Munkerup, M. Thulin, D. Tan, X. Lim, R. Lee and K. W. Huang, Importance of thorough conformational analysis in

modelling transition metal-mediated reactions: Case studies on pincer complexes containing phosphine groups, *J. Saudi Chem. Soc.*, 2019, **23**, 1206–1218.

18 A. K. Vitek, T. M. E. Jugovic and P. M. Zimmerman, Revealing the Strong Relationships between Ligand Conformers and Activation Barriers: A Case Study of Bisphosphine Reductive Elimination, *ACS Catal.*, 2020, **10**, 7136–7145.

19 J. Bartol, P. Comba, M. Melter and M. Zimmer, Conformational searching of transition metal compounds, *J. Comput. Chem.*, 1999, **20**, 1549–1558.

20 M. Besora, A. A. C. Braga, G. Ujaque, F. Maseras and A. Lledós, The importance of conformational search: A test case on the catalytic cycle of the Suzuki-Miyaura cross-coupling, *Theor. Chem. Acc.*, 2011, **128**, 639–646.

21 D. Suárez, N. Díaz and R. Lõpez, A combined semiempirical and DFT computational protocol for studying bioorganometallic complexes: Application to molybdocene-cysteine complexes, *J. Comput. Chem.*, 2014, **35**, 324–334.

22 D. Suárez and N. Díaz, Molecular modeling of bioorganometallic compounds: Thermodynamic properties of molybdocene-glutathione complexes and mechanism of peptide hydrolysis, *Chem. Phys. Chem.*, 2015, **16**, 1646–1656.

23 A. K. Rappé, C. J. Casewit, K. S. Colwell, W. A. Goddard III and W. M. Skiff, UFF, a Full Periodic Table Force Field for Molecular Mechanics and Molecular Dynamics Simulations, *J. Am. Chem. Soc.*, 1992, **114**, 10024–10035.

24 A. K. Rappé, K. S. Colwell and C. J. Casewit, Application of a Universal Force Field to Metal Complexes, *Inorg. Chem.*, 1993, **32**, 3438–3450.

25 P. O. Norrby and P. Brandt, Deriving force field parameters for coordination complexes, *Coord. Chem. Rev.*, 2001, **212**, 79–109.

26 P. Comba and R. Remenyi, Inorganic and bioinorganic molecular mechanics modeling - The problem of the force field parameterization, *Coord. Chem. Rev.*, 2003, **238–239**, 9–20.

27 D. Troya, Reactivity Consequences of Conformational Isomerism in 1-Propanol, *J. Phys. Chem. A*, 2019, **123**, 1044–1050.

28 D. I. Sharapa, A. Genaev, L. Cavallo and Y. Minenkov, A Robust and Cost-Efficient Scheme for Accurate Conformational Energies of Organic Molecules, *Chem. Phys. Chem.*, 2019, **20**, 92–102.

29 C. Duan, D. B. K. Chu, A. Nandy and H. J. Kulik, Detection of multi-reference character imbalances enables a transfer learning approach for virtual high throughput screening with coupled cluster accuracy at DFT cost, *Chem. Sci.*, 2022, **13**, 4962–4971.

30 C. R. Groom, I. J. Bruno, M. P. Lightfoot and S. C. Ward, The Cambridge structural database, *Acta Crystallogr., Sect. B: Struct. Sci., Cryst. Eng. Mater.*, 2016, **72**, 171–179.

31 F. Neese, The ORCA program system, *Wiley Interdiscip. Rev.: Comput. Mol. Sci.*, 2012, **2**, 73–78.

32 F. Neese, Software update: The ORCA program system—Version 5.0, *WIREs Comput. Mol. Sci.*, 2022, e1606.

33 S. Grimme and A. Hansen, A Practicable Real-Space Measure and Visualization of Static Electron-Correlation Effects, *Angew. Chem., Int. Ed.*, 2015, **54**, 12308–12313.

34 J. P. Perdew, K. Burke and M. Ernzerhof, Generalized gradient approximation made simple, *Phys. Rev. Lett.*, 1996, **77**, 3865–3868.

35 J. P. Perdew, K. Burke and M. Ernzerhof, Erratum: Generalized gradient approximation made simple (Physical Review Letters (1996) 77 (3865)), *Phys. Rev. Lett.*, 1997, **78**, 1396.

36 D. N. Laikov, A new class of atomic basis functions for accurate electronic structure calculations of molecules, *Chem. Phys. Lett.*, 2005, **416**, 116–120.

37 D. N. Laikov and Y. A. Ustynyuk, PRIRODA-04: A quantum-chemical program suite. New possibilities in the study of molecular systems with the application of parallel computing, *Russ. Chem. Bull.*, 2005, **54**, 820–826.

38 C. Riplinger and F. Neese, An efficient and near linear scaling pair natural orbital based local coupled cluster method, *J. Chem. Phys.*, 2013, **138**, 34106.

39 C. Riplinger, B. Sandhoefer, A. Hansen and F. Neese, Natural triple excitations in local coupled cluster calculations with pair natural orbitals, *J. Chem. Phys.*, 2013, **139**, 134101.

40 C. Riplinger, P. Pinski, U. Becker, E. F. Valeev and F. Neese, Sparse maps - A systematic infrastructure for reduced-scaling electronic structure methods. II. Linear scaling domain based pair natural orbital coupled cluster theory, *J. Chem. Phys.*, 2016, **144**, 24109.

41 F. Weigend and R. Ahlrichs, Balanced basis sets of split valence, triple zeta valence and quadruple zeta valence quality for H to Rn: Design and assessment of accuracy, *Phys. Chem. Chem. Phys.*, 2005, **7**, 3297–3305.

42 C. Adamo and V. Barone, Toward reliable density functional methods without adjustable parameters: The PBE0 model, *J. Chem. Phys.*, 1999, **110**, 6158–6170.

43 S. Grimme, J. Antony, S. Ehrlich and H. Krieg, A consistent and accurate ab initio parametrization of density functional dispersion correction (DFT-D) for the 94 elements H-Pu, *J. Chem. Phys.*, 2010, **132**, 154104–154119.

44 S. Grimme, S. Ehrlich and L. Goerigk, Effect of the damping function in dispersion corrected density functional theory, *J. Comput. Chem.*, 2011, **32**, 1456–1465.

45 Y. Zhao and D. G. Truhlar, The M06 suite of density functionals for main group thermochemistry, thermochemical kinetics, noncovalent interactions, excited states, and transition elements: Two new functionals and systematic testing of four M06-class functionals and 12 other function, *Theor. Chem. Acc.*, 2008, **120**, 215–241.

46 N. Mardirossian and M. Head-Gordon, ωb97X-V: A 10-parameter, range-separated hybrid, generalized gradient approximation density functional with nonlocal correlation, designed by a survival-of-the-fittest strategy, *Phys. Chem. Chem. Phys.*, 2014, **16**, 9904–9924.

47 K. G. Dyall, An exact separation of the spin-free and spin-dependent terms of the Dirac-Coulomb-Breit Hamiltonian, *J. Chem. Phys.*, 1994, **100**, 2118–2127.

48 S. Grimme, J. G. Brandenburg, C. Bannwarth and A. Hansen, Consistent structures and interactions by density functional theory with small atomic orbital basis sets, *J. Chem. Phys.*, 2015, **143**, 54107.

49 J. G. Brandenburg, C. Bannwarth, A. Hansen and S. Grimme, B97-3c: A revised low-cost variant of the B97-D density functional method, *J. Chem. Phys.*, 2018, **148**, 064104.
50 J. J. P. Stewart, Optimization of parameters for semiempirical methods V: Modification of NDDO approximations and application to 70 elements, *J. Mol. Model.*, 2007, **13**, 1173–1213.
51 J. J. P. Stewart, Optimization of parameters for semiempirical methods VI: More modifications to the NDDO approximations and re-optimization of parameters, *J. Mol. Model.*, 2013, **19**, 1–32.
52 J. J. P. Stewart, *MOPAC2016; Stewart Computational Chemistry*, Colorado Springs, CO, USA, 2016. **https://openmopac.net** (accessed March 25, 2022).
53 S. Grimme, C. Bannwarth and P. Shushkov, A Robust and Accurate Tight-Binding Quantum Chemical Method for Structures, Vibrational Frequencies, and Noncovalent Interactions of Large Molecular Systems Parametrized for All spd-Block Elements (Z = 1-86), *J. Chem. Theory Comput.*, 2017, **13**, 1989–2009.
54 C. Bannwarth, S. Ehlert and S. Grimme, GFN2-xTB - An Accurate and Broadly Parametrized Self-Consistent Tight-Binding Quantum Chemical Method with Multipole Electrostatics and Density-Dependent Dispersion Contributions, *J. Chem. Theory Comput.*, 2019, **15**, 1652–1671.
55 S. Spicher and S. Grimme, Robust Atomistic Modeling of Materials, Organometallic, and Biochemical Systems, *Angew. Chem., Int. Ed.*, 2020, **59**, 15665–15673.
56 C. Bannwarth, E. Caldeweyher, S. Ehlert, A. Hansen, P. Pracht, J. Seibert, S. Spicher and S. Grimme, Extended tight-binding quantum chemistry methods, *Wiley Interdiscip. Rev.: Comput. Mol. Sci.*, 2021, **11**, e1493.
57 M. Atanasov, D. Ganyushin, D. A. Pantazis, K. Sivalingam and F. Neese, Detailed Ab initio first-principles study of the magnetic anisotropy in a family of trigonal pyramidal iron(II) pyrrolide complexes, *Inorg. Chem.*, 2011, **50**, 7460–7477.
58 M. Atanasov, J. M. Zadrozny, J. R. Long and F. Neese, A theoretical analysis of chemical bonding, vibronic coupling, and magnetic anisotropy in linear iron(ii) complexes with single-molecule magnet behavior, *Chem. Sci.*, 2013, **4**, 139–156.
59 M. Dolg, U. Wedig, H. Stoll and H. Preuss, Energy-adjusted ab initio pseudopotentials for the first row transition elements, *J. Chem. Phys.*, 1986, **86**, 866–872.

